

A new charged particle detector for the KOTO experiment at J-PARC

HongMin KIM for the KOTO Collaboration

Division of Science Education, Jeonbuk National University, Jeonju 54896, Republic of Korea

E-mail: recenter@naver.com

Abstract. We report the performance of a new scintillator array Downstream Charged Veto (DCV) for the J-PARC KOTO experiment to suppress the $K_L \rightarrow \pi^+ \pi^- \pi^0$ decay background. Since the background originates from undetected charged pions passing through the beam hole of the electromagnetic calorimeter, the DCV detector was installed in vacuum downstream of the calorimeter. The DCV is composed of two plastic scintillator pipes read out by Multi Pixel Photon Counters (MPPCs) through wavelength shifting (WLS) fibers. The light yield was found to be 60 photoelectrons/0.8 MeV in a test bench when cosmic-rays pass through the center of the DCV. Energy calibration was performed using cosmic-rays after installation.

1. Introduction

The KOTO experiment at J-PARC aims to study the $K_L \rightarrow \pi^0 \nu \bar{\nu}$ decay, which is one of the most sensitive probes to new physics beyond the standard model (SM). Its signature is a pair of photons from a π^0 decay without any additional activity in the hermetic detector system surrounding the decay region. To detect this highly suppressed decay, expected at 3×10^{-11} in the SM, it is important to reject background events related to other kaon decay modes. At the single event sensitivity of 1.30×10^{-9} achieved with 2015 data by KOTO, the number of $K_L \rightarrow \pi^+ \pi^- \pi^0$ background events was estimated to be 0.05 [1], which corresponds to 2 events at the SM sensitivity. The decay becomes background when charged pions passing through the beam hole are undetected due to their interaction with non-active materials. A Monte Carlo simulation shows that most of π^+ and π^- particles disappear in three sections, as illustrated in Fig. 1. One is the membrane which separates the 10^{-5} Pa decay region and the 0.1 Pa detector region. Another source is square pipes made of 0.5-mm-thick G10 plates placed inside the calorimeter and the CC04 separately, which prevents the membrane from drooping toward the beam axis. The last one is a beam pipe made of 10-mm-thick aluminum for extending the vacuum region downstream.

To suppress the $K_L \rightarrow \pi^+ \pi^- \pi^0$ background, such charged pions should be detected before they interact with those non-active materials. In this respect, we decided to install a new charged particle detector, named DCV, inside the high vacuum region downstream of the electromagnetic calorimeter. To maximize the detector performance, the DCV should be placed as close as possible to the calorimeter. Since the DCV is able to support the membrane, we do not need the G10-pipe inside the CC04 anymore. The G10-pipe placed inside the calorimeter is still needed, though its length can be shortened.

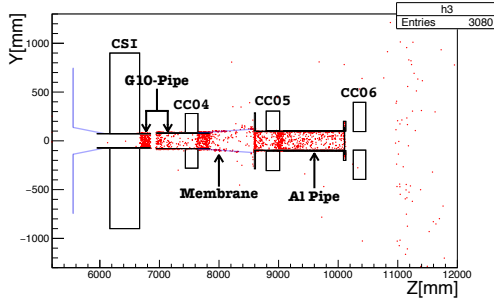


Figure 1. Interacting points of π^+ and π^- . Red dots indicate where the charged pions are disappeared.

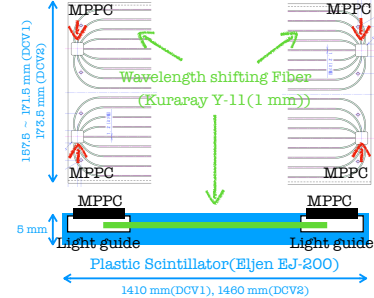


Figure 2. Configuration of scintillator with WLS fibers and MPPCs.

32 **2. Structure of the DCV**

33 The DCV consists of two successive square pipes, and each of them is made of 4 sheets of
 34 scintillators. The DCV1 is placed at 463 mm downstream from the calorimeter and inside the
 35 membrane, and the DCV2 is placed at 76 mm downstream from the DCV1 and inside the
 36 aluminum beam pipe. The DCV1 is a 1410-mm-long tapered square pipe with cross sections of
 37 157.5 mm square at the upstream end and 171.5 mm square at the downstream end. The DCV2
 38 is a 1460-mm-long square pipe with a side length of 173.5 mm. WLS fibers (Y11, Kuraray) with
 39 a diameter of 1 mm are embedded in 18 parallel grooves in a 5-mm-thick plastic scintillator
 40 (EJ-200, Eljen Technology). Due to the limited space for the DCV, we needed to attach the
 41 MPPCs on the scintillator surface directly. An aluminum light guide for the MPPCs is placed
 42 in both ends of the scintillator, and the WLS fibers are routed into the light guide. Since the
 43 size of the light guide is $6 \times 6 \text{ mm}^2$ to fit the size of MPPC, the WLS fibers should be bent
 44 to converge into the light guide as shown in Fig. 2. The curvature of grooves near the end
 45 of scintillator is designed to have a radius larger than 20 mm. The light loss increases rapidly
 46 below the radius of 20 mm, as illustrated in Fig. 3. The WLS fibers are grouped into two and
 47 read by MPPC (S13360-6050PE, Hamamatsu) at both ends of each group (4 read-out MPPCs
 48 in total).

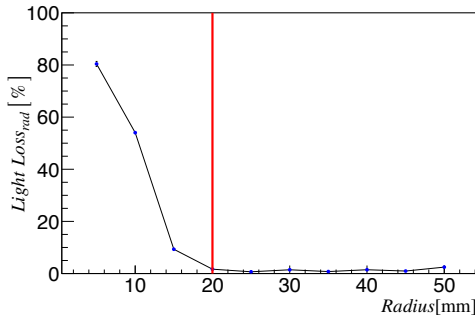


Figure 3. Light loss due to the curvature of the WLS fiber.

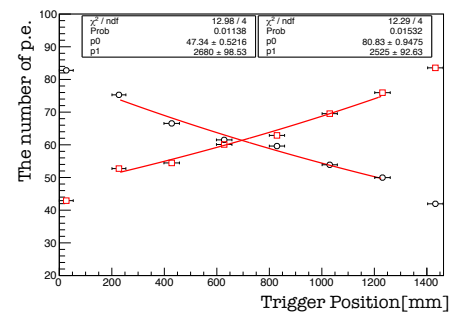


Figure 4. Number of photoelectrons at each cosmic-ray trigger point.

49 **3. Fabrication Process**

50 The WLS fibers were glued to the plastic scintillator plate using the optical cement (BC-600, 51 Saint-Gobain) and introduced to the light guide at the both ends of the plate. The soundness 52 of all WLS fibers were tested by measuring light yield at one end of the fibers while an LED 53 light (430 nm) illuminated at their other end. After waiting for 48 hours for the optical cement 54 to be hardened enough, we placed the scintillator in < 1 Pa vacuum for more than 48 hours 55 to extract outgas from the glued scintillators. The scintillators were wrapped by a 12- μm -thick 56 aluminized mylar, and the MPPCs were respectively attached to the light guide and were fixed 57 by aluminum plates.

58 Four MPPCs are attached to each side of the DCV scintillator and operated at a common 59 high voltage. A MPPC gain was measured using a single photoelectron spectrum to group 60 MPPCs with similar gains.

61 The light yield of the assembled scintillator was measured by using cosmic-rays triggered at 62 eight different positions of the plates. As shown in Fig. 4, the average number of photoelectrons 63 for 0.8 MeV energy deposited by cosmic-rays hitting the center of the scintillator was 60.2 for 64 the DCV1 and 58.6 for the DCV2. The light attenuation lengths were (2469 ± 165.1) mm for 65 the DCV1 and (2566 ± 166.0) mm for the DCV2, respectively.

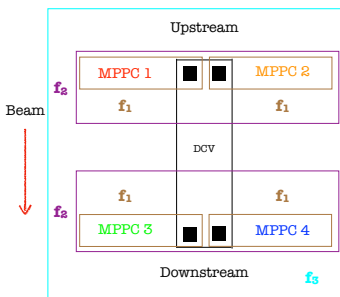


Figure 5. Three different gain factors for the DCV energy calibration with 4 MPPCs.

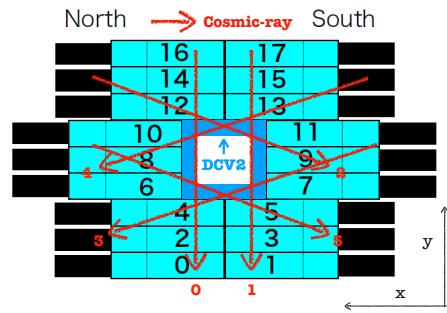


Figure 6. Tracks of the cosmic-rays identified by the CC05 for the DCV2 calibration.

66 **4. Energy Calibration**

67 After the installation of the DCV, we took the cosmic-ray data for its energy calibration. We 68 used two detectors made of CsI crystals and surrounding the DCV (i.e. the CC04 for the DCV1 69 and the CC05 for the DCV2) as the trigger counter. We can select a track of the cosmic-ray 70 by using the detectors as shown in Fig. 6, and estimate the amount of energy deposits by the 71 cosmic-ray in the DCV. Since the scintillation light was shared by 4 MPPCs, we needed to 72 extract gain factors for them to produce an energy deposit after summing up. As the first step, 73 we selected the tracks passing through only half parts of the DCV in which a clear peak in the 74 ADC distribution can be obtained at single MPPC. For example, track 1 was used to get the 75 ADC distribution for MPPCs placed at the south parts of the top and bottom plates. After 76 fitting the Landau distribution convoluted with Gaussian to the obtained ADC distributions 77 of each MPPC, we evaluated the gain factor f_1 from the MPV value for them individually. 78 Secondly, we corrected for the effect of shower sharing (f_2) by summing up calibrated ADC 79 values with the f_1 for two MPPCs at both ends individually and fitted again the same function. 80 Finally, we summed 4 calibrated ADC values applied the two factors (f_1 and f_2) at the same 81 time and fitted again to obtain the gain factor, f_3 .

82 During the beam time from February to April in 2019, we collected the cosmic-ray data at the
 83 accelerator maintenance day once in a week. Figure 7 shows gain factors for whole MPPCs and
 84 variation according to time of data taking. The gain factors tend to increase over time which
 85 implies that the gains of MPPCs decrease. A detailed study on the variation is undergoing.

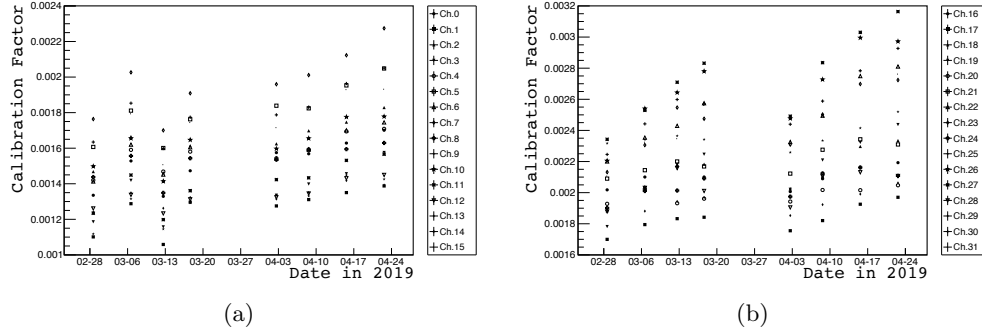


Figure 7. Calibration Factor over time for DCV1 (a) and DCV2 (b).

86 5. Summary

87 We fabricated and installed a new charged particle detector DCV for further rejection of the
 88 background events from the $K_L \rightarrow \pi^+\pi^-\pi^0$ decay. Based on the cosmic-ray test performed
 89 during its fabrication, the light yield is 60 photoelectrons for 0.8 MeV energy deposit at the
 90 center of the DCV. We established a method of its calibration by using cosmic-ray identified
 91 by detectors surrounding the DCV. Long-term stability of the DCV performance is now under
 92 study.

93 Acknowledgements

94 This work is supported by the National Research Foundation of Korea-2017R1A2B4006359,
 95 and the JSPS KAKENHI Grant No. JP23224007 and No.17K05480.

96 Reference

97 [1] J.K. Ahn *et al.* (KOTO Collaboration) 2019, *Phys. Rev. Lett.* **122** 021802.